Thermo-mechanical toner transfer for high-quality digital image correlation speckle patterns

Paolo Mazzoleni [a], Emanuele Zappa [b,*], Fabio Matta [c], Michael A. Sutton [d]

[a] Rolls-Royce, Pride Park, Derby DE24 8LY, UK
[b] Department of Mechanical Engineering, Politecnico di Milano, via La Masa 1, 20156 Milan, Italy
[c] Department of Civil and Environmental Engineering, University of South Carolina, 300 Main Street, Columbia, SC 29208, USA
[d] Department of Mechanical Engineering, University of South Carolina, 300 Main Street, Columbia, SC 29208, USA

Received 5 January 2015
Received in revised form
18 May 2015
Accepted 29 June 2015
Available online 21 July 2015

1. Introduction

The surface of a specimen must provide sufficient variation in contrast to ensure that the full-field displacements measured using digital image correlation (DIC) [1,2] are accurate. Typically an artificial speckles are applied to a surface to obtain a high contrast random pattern. Recent studies have shown that the frequency content of the speckle pattern affects the accuracy [3–9] and spatial resolution [10,11] of DIC measurements for a given test setup and equipment. While there are no general mathematical formulations to define effective speckle patterns, extensive research has highlighted salient characteristics. For example, an average speckle diameter of a few pixels is required to minimize aliasing effects in the correlation analysis, while ensuring good spatial resolution (e.g., sampling of each feature by at least 3×3 pixels [1] or by 2×2 to 5×5 pixels [5]). Lecompte et al. [4] presented a quantitative evaluation of DIC measurement accuracy with respect to mean speckle size and subset dimension, high-lighting the importance of selecting suitable combinations of speckle and subset size, while tailoring the subset size to the expected deformation field. Pan et al. [7] examined different speckle patterns with respect to measurement accuracy (bias error) and precision (standard deviation error). Lecompte et al.[6] investigated the effect of the speckle-to-surface area ratio (coverage factor) and, for a 15×15 pixel subset, demonstrated that the optimal speckle size is 5×5 pixels and the optimal coverage lies between 40% and 70%. Pan et al. [3] proposed an alternative approach where the average pattern gradient is related to both bias and standard deviation of the error, in agreement with Wang et al. [12].

Depending on the surface material and specimen size, different patterning methods may be required. In many cases, it is challenging to implement the practical recommendations reported in the literature to create effective speckle patterns. Spray painting using airbrushes is the most common technique for specimen sizes in the range $\sim$1 mm to $\sim$100 mm (e.g., [1,13,14]). In fact, speckle size can be controlled in a simple and practicable fashion through a combination of ink viscosity, nozzle size and spray distance, while the density of speckles can be adjusted based on spraying time. However, for specific applications (e.g., on relatively large regions of interest as in the examples in Fig. 1 [15,16]), the need to create speckle patterns with particles having well-defined and consistent shape, size and spacing (e.g., [9,17]) has prompted the

* Corresponding author. Tel.: +39 02 23998445; fax: +39 02 23998585.
E-mail addresses: paolomazzoleni@yahoo.it (P. Mazzoleni), emanuele.zappa@polimi.it (E. Zappa), fmatta@sc.edu (F. Matta), sutton@sc.edu (M.A. Sutton).

development and implementation of other suitable techniques. For example, Helm [18] used a stamp made from a steel plate covered with a pattern of felt disks to create speckles with a diameter of approximately 10 mm on the 2.1 × 2.1 m^2 surface of a reinforced concrete slab. Ghorbani et al. [15] used flexible polymer stencils to spray paint numerically-designed speckle patterns on the surface of full-scale concrete and masonry walls. Here, the use of relatively large speckles, for which spray painting is impractical, becomes necessary to ensure a suitable balance between measure-ment accuracy and spatial resolution, enabling the identification of faithful crack maps at any given loading stage [15]. For the case of smaller regions of interest, El-Hajjar and Petersen [19] demonstrated the use of laser-printed adhesive polyvinyl chloride coatings on fiber-reinforced polymer coupons, and applications based on stamping [20,21] and other techniques [22,23] have been reported.

This paper introduces a novel technique to create speckle patterns for DIC measurements by means of a thermo-mechanical process where melted toner is transferred from printed paper onto the measurement surface. The proposed technique, which is widely exploited in the manufacturing process for low-cost electronic printed circuit boards, enables the creation of patterns with consistent speckle size and density in a repeatable, simple, rapid and inexpensive fashion. First, the procedure is presented in detail. Then, the tuning and quantitative quality assessment of the resulting speckle patterns are discussed, together with the applicability to different materials and surfaces. Finally, proof of concept is demonstrated for (a) a welded steel plate subjected to uniaxial tensile loading, and (b) an aluminum plate exposed to different temperatures up to 451 °C, i.e., relatively high temperatures for which specialized patterning techniques need to be enlisted (e.g., [24]).

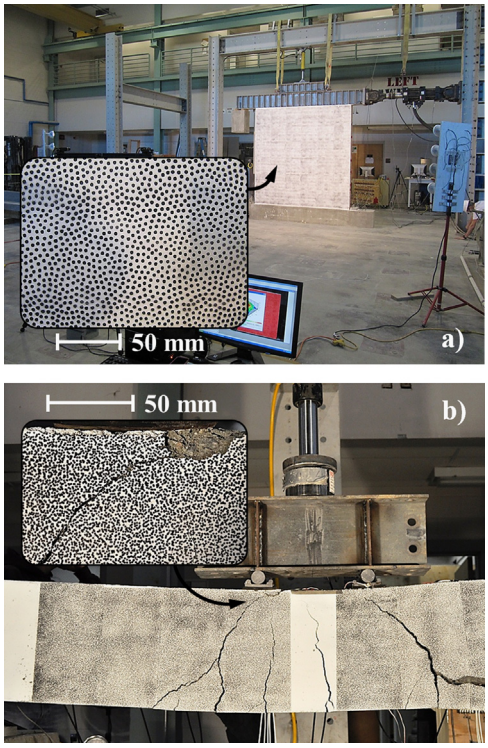

Fig. 1. Numerically-designed speckle pattern on large-scale concrete specimens: (a) 2.4 × 2.5 m^2 concrete masonry wall surface [15]; and (b) 330 mm deep reinforced concrete beam [16].

2. Methodology

The desired speckle pattern is numerically designed, printed on paper using a conventional laser printer, and then thermo-mechanically transferred onto the measurement surface. These three steps are detailed as follows.

2.1. Speckle pattern design

Circular speckles are used to minimize local features associated with preferential directions. An ordinate grid of speckles with a given diameter and on-center spacing is numerically generated (Fig. 2a). The ordinate grid is then perturbed by adding to the horizontal and vertical coordinates of each speckle a random amount of noise, which is extracted from a normal distribution. The resulting patterns (Fig. 2b) are approximately spatially isotropic for the subset sizes used in the proof-of-concept experiments presented herein (i.e., 21 × 21 pixels and 41 × 41 pixels). The strategy of perturbing an ordinate grid instead of randomly positioning the speckles on a given surface area aims at providing a more homogeneous speckle distribution. In the examples pre-sented in this paper, a 4.5 pixel speckle diameter is used as it lies in the desirable range of 2–5 pixels [5]. The original on-center spacing of the speckles in the ordinate grid is 6 pixels (Fig. 2a). The horizontal and vertical coordinates of each speckle are then perturbed by adding random values in the range ±2.5 pixels (Fig. 2b). The resulting coverage factor is 42%, which lies in the recommended range of 40–70% [6].

Dark speckles on a light background without intermediate gray levels are used to maximize contrast and thus measurement signal-to-noise ratio. It is noted that this does not imply a binary color distribution in the image acquired by the camera as the filtering of the camera optics softens the dark-to-light transition, resulting in a blurring of the speckle edges (Fig. 2c).

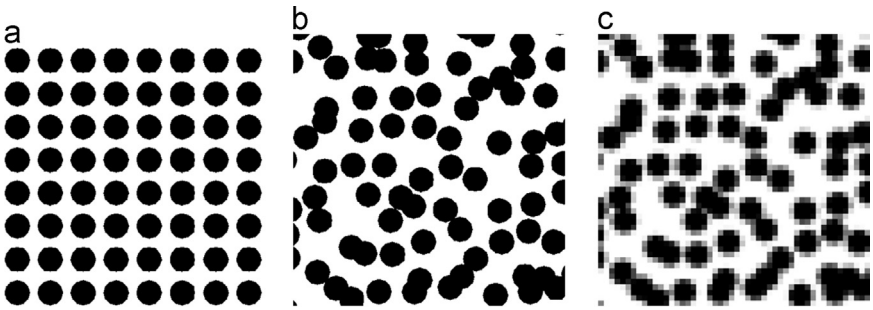

Fig. 2. Design of speckle pattern: (a) original ordinate grid; (b) random pattern; and (c) downsampled random pattern representative of pattern framed by camera.

2.2. Printing on paper

The speckle pattern designed is first printed on paper. The ratio between camera resolution (pixels) and measurement area (millimeters) dictates the mm-to-pixel scaling factor. An inexpensive laser printer can be used, although smaller scaling factors may require printers with a higher dpi resolution. As an alternative, the pattern can be printed using an inkjet printer and photocopied using a laser copy machine. In this study, a laser printer (model T653, Lexmark, Lexington, KY) was used. The highest quality printout is set and a test page is printed to warm-up the machine. The paper must be carefully selected to allow the toner to (1) melt during printing without smudging; and (2) print the speckle pattern on the paper surface making it possible to impress it on the measurement surface in the following step. To this end, glossy photographic paper suitable for inkjet printers was used for proof of concept in this study. The use of different types of paper (e.g., linen paper) or printer (e.g, inkjet printer) should be verified on a case-by-case basis.

2.3. Toner transfer onto measurement surface

The measurement surface must be clean and relatively smooth (i. e., sufficiently rough to facilitate adhesion of the enamel paint that may be used to obtain a high contrast background). Suitable examples range from metallic surfaces cleaned with acetone and with surface roughness typical of machined surfaces, to sandblasted metals and concrete, as discussed as part of the proof of concept presented in Section 3. A thin layer of white opaque (i.e., for indoor use) enamel should be sprayed on all relatively dark or reflecting surfaces to increase contrast and minimize reflections (the toner itself is opaque), respectively. In particular, the enamel layer facilitates toner transfer onto glossy or porous surfaces (e.g., concrete). A brittle (e.g., silicon-less) enamel is preferable to detect cracks in the underlying surface rather than measuring large but inaccurate deformations.

To enable an effective toner transfer, the printed paper must be placed onto the specimen and then heated while applying a uniform pressure, such that the toner on the paper re-melts and is transferred onto the surface of the specimen. Heating the paper to 100 °C is suitable as toner powders typically melt at 70–90 °C [25]. In this study, a common flatiron is used for this operation together with a cloth that is inserted between the hot surface and the printed paper to facilitate the contact between the specimen surface and the paper. When transferring the speckle pattern onto curved surfaces, inserting a multi-layer cloth may be considered for better pressure distribution. The time required for toner transfer depends on the thickness of the specimen and the thermal conductivity of the surface material. In this study, three minutes were sufficient to impress the speckle pattern onto the surface of a 5-mm thick aluminum plate. Then, the specimen was cooled in cold water, which also facilitated the removal of the paper without imparting any visible damage to the speckle pattern. Operating on curved surfaces is more time-consuming as it is necessary to rotate the heating source along the measure-ment surface. However, it is also noted that spray painting becomes more complex on curved surfaces as the curvature increases. Different approaches to heat the paper and allow toner transfer can be considered for specimen surfaces that are larger than a typical flatiron. For example, the paper and cloth may be covered with a metallic (e.g., aluminum) plate, using a heat source (e.g., flame gun) to increase the temperature to the desired level.

3. Proof of concept

The proof of concept consists in the tuning of the speckle size, the quantitative quality assessment of the resulting speckle pattern, and the demonstration of the proposed toner-transfer technique in two examples.

3.1. Tuning of speckle size

Throughout the printing and toner-transferring process, a difference may arise between the size of the designed speckles and those actually impressed (toner-transferred) onto the measurement surface. Speckle sizes in the range 2–5 pixels can be effectively used for the purpose of DIC analysis [5]. However, in order to consistently obtain speckles with a diameter as close as possible to the design value, the difference in size between designed and toner-transferred speckles should be characterized and compensated for. In addition, by systematically quantifying the difference between designed and toner-transferred speckle diameter for different design (nominal) speckle sizes, the speckle pattern for a given application can be more rationally selected. The tuning process is demonstrated as follows.

Ordinate grids of speckles, each having a different nominal diameter ranging from 1.0 to 0.05 mm (where the latter is the smallest size that can be printed with the machine used in this study), were designed, printed, and impressed on 50 × 50 mm^2 aluminum surfaces. A 5-mm thick aluminum sample was used for each speckle size. For the nominal speckle diameter of 1.0 mm, the printed surface included 500 speckles spaced at 2.0 mm (i.e., two times the nominal diameter) on-center. For the nominal speckle diameter of 0.05 mm, the printed surface included in excess of 90,000 speckles spaced at 0.15 mm on-center (i.e., three times the nominal diameter to offset the tendency of the toner to smudge, resulting in speckles that are larger than those designed). The patterned surfaces were then scanned with a high-resolution (4800 dpi) document scanner and an image processing technique known as “particle analysis” [26] was performed on the images. The resulting images were characterized by circular speckles with diameter equal to or greater than 28 pixels, i.e., sufficiently large to be essentially unaffected by uncertainty in diameter estimation.

Particle analysis [26] enables the detection of regions of an image with homogeneous gray levels (in this case the dark speckles) and the estimation of the salient geometric properties of each particle (speckle), such as area and diameter. For a given nominal (design) speckle size, the equivalent diameter of each speckle transferred onto the plate, defined as the diameter of a circle having an equivalent area to that of the speckle, was computed. Fig. 3 illustrates the relation between the nominal diameter in the range 0.05–1.0 mm and the resulting average equivalent diameter (along with the standard deviation) as obtained via toner-transfer onto the aluminum surface. The average difference between nominal and toner-transferred diameter consistently decreases for larger speckles, namely from 0.15 mm for 0.05 mm speckles to 0.05 mm for 1.0 mm speckles. While this difference depends on the specific printer and paper

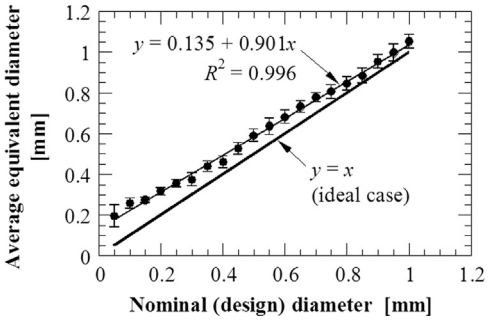

Fig. 3. Relation between nominal (design) and average equivalent (transferred) speckle diameter on aluminum sample.

used, the results reported in Fig. 3 are representative of those that can be obtained using a professional laser printer and glossy photographic paper. In fact, as the speckle size is reduced and the limit of the printer resolution is approached, the printed speckles tend to be larger than those designed especially when using paper where the toner can more easily spread before drying. In this study, the linear regression function indicated in Fig. 3 is used to compensate for the difference between nominal and toner-transferred speckle diameter. The minimum speckle size that can be transferred is approximately 0.2 mm, which is associated with a design value of 0.05 mm (Fig. 3). The difference between design and impressed diameter is due to the smudging of the toner, whose effect is reduced as the speckle size is increased. However, from a practical standpoint, alternative techniques such as spray painting through patterned stencils may be more convenient when larger speckles are required, and when extensive regions of interest need to be patterned (e.g., [15]).

The calibration results shown in Fig. 3 demonstrate that, when designing a speckle pattern for toner transfer, it is feasible to compensate for the systematic effect of toner smudging on the speckle size. In addition, some practical measures can be considered to minimize this systematic effect, including: controlling the temperature at which toner transfer occurs as viscosity is reduced at increasing temperatures [25], thus facilitating toner smudging (a temperature of 100 °C is recommended); and, limiting the time for toner transfer to a minimum (three to four minutes and about two minutes are recommended for high-thermal conductivity materials such as metals and low-thermal conductivity materials such as concrete, respectively).

3.2. Quality assessment of speckle pattern

The speckle pattern shown in Fig. 2b was printed in four different scales, ranging from 3.75 to 15 pixel/mm, using a nominal speckle diameter of 4.5 pixels. For each scale, the pattern was impressed on the 50×50 mm^2 surface of a 5-mm thick aluminum sample. The surface was previously degreased with acetone and spray-painted with white opaque enamel to enhance the pattern contrast. The scaling factor, nominal and average equivalent speckle diameter for each specimen (denoted as "A" through "D") is reported in Table 1. The specimens were framed with a gray-scale, eight-bit digital camera preserving the scaling factors in Table 1, and preventing the local saturation of the camera sensor during image acquisition. Fig. 4 shows the image of a 100×100 pixel sample for each scaled pattern, where the quality of the result in terms of contrast, detail and uniformity can be noted.

The mean intensity gradient (MIG) coefficient introduced by Pan et al. [3] was enlisted to quantitatively assess the quality of the scaled speckle patterns shown in Fig. 4. The modulus of the local intensity gradient vector of a gray-scale image is defined as per Eq. (1):

$$|\nabla f(x_{ij})| = \sqrt{f_x(x_{ij})^2 + f_y(x_{ij})^2} \tag{1}$$

where $f_x(x_{ij})$ and $f_y(x_{ij})$ are the x- and y-directional intensity derivatives at pixel x_{ij}, as computed using the central difference method. The MIG coefficient is thus defined as per Eq. (2):

$$\mathrm{MIG} = \sum_{i=1}^{W} \sum_{j=1}^{H} \frac{|\nabla f(x_{ij})|}{WH} \tag{2}$$

where W and H are the image width and height (in pixels), respectively. It is noted that a slightly different form of Eq. (2) was originally identified by Wang et al. [12] as the primary measure of subset contrast in image correlation, and was later used by Pan et al. [3] in the form shown in Eq. (2) as an effective means to assess the quality of a DIC speckle pattern. In fact, higher MIG values typically result in smaller bias and less dispersion in the DIC measurements [3]. The MIG value for the four scaled speckle patterns is indicated in Fig. 4. Speckle patterns A and C have similar MIG values (46.9 and 46.6, respectively), whereas similar but smaller values characterize speckle patterns B and D (41.8 and 40.1, respectively), where the difference may be due to a soft blurring in the acquired images. However, all speckle patterns are characterized by a MIG value greater than 40, and higher than the most effective high-contrast spray-painted pattern tested by Pan et al. [3]. In addition, high MIG values in spray painted speckle patterns may be attained despite the presence of low-contrast areas having a relatively small number of speckles or high speckle clustering, thus making local inspections necessary [10,11]. The proposed toner-transfer technique offsets this drawback since the characteristics of the speckle pattern are controlled as it is numerically designed.

While quality assessment is demonstrated herein as a proof-of-concept for a specific speckle pattern (and for four scaling factors), it is noted that virtually any speckle pattern can be produced via toner transfer after optimizing the design by maximizing the MIG coefficient.

Table 1
Scaling factor of speckle patterns on aluminum surfaces.

Speckle pattern	Scaling factor [pixel/mm]	Nominal speckle diameter [mm]	Average equivalent speckle diameter [mm]
A	3.75	1.20	1.22
B	5.00	0.90	0.95
C	7.50	0.60	0.68
D	15.0	0.30	0.38

3.3. Applicability of toner-transfer technique

The main limitation of the toner-transfer technique is that it can be implemented on surface materials that can be heated to about 100 °C for a few minutes without producing physical damage or altering relevant mechanical properties. For example, the technique is not suitable for polymer matrix composites whose glass transition temperature lies below 100 °C, whereas it lends itself to applications on cement composites (e.g., concrete as shown in Fig. 5a) and metallic alloys (e.g., aluminum as shown in Fig. 5b). It is also noted that some surface roughness, for example similar to that of machined metallic surfaces, is necessary to facilitate toner transfer (e.g., by preventing smudging). The technique can be conveniently used to impress speckle patterns on curved surfaces using a suitable heating source, such as in the case of concrete cylinders used for mechanical characterization under uniaxial compression force (e.g., [27,28]) and metallic specimens (e.g., Fig. 5b).

For large specimens such as the full-scale masonry wall in Fig. 1a [15] and the reinforced concrete beam in Fig. 1b [16], where the speckle patterns were impressed via spray painting through flexible stencils, it is viable to use the toner-transfer technique for relatively small areas of interest. Otherwise, patterning the entire surface becomes labor intensive and time consuming, and the required scaling factor may call for relatively larger speckles that can be more conveniently painted using stencils (e.g., [15]). For small measure-ment surfaces, the minimum speckle size depends on the capabilities of the printer used. For the printer used in this study, as verified as part of the toner-transfer tuning, a minimum equivalent speckle diameter of 0.2 mm is obtained using a nominal (design) diameter of 0.05 mm (Fig. 3). For an equivalent diameter of 4.5 pixels, the scaling factor is 22.5 pixel/mm, thus enabling DIC measurements on a framed area of 63×63 mm^2 using a two-megapixel camera. Based

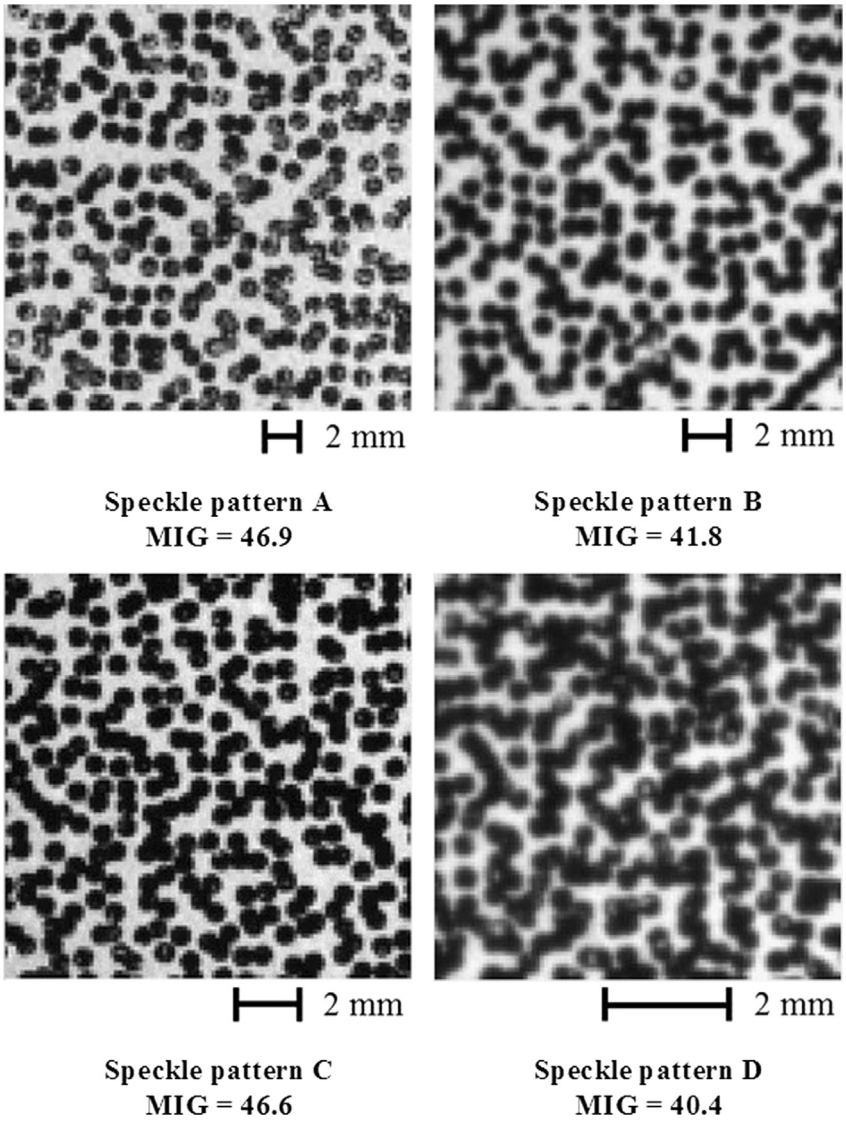

Fig. 4. Scaled speckle patterns as transferred onto aluminum surfaces (100 × 100 pixel samples) and associated MIG coefficients.

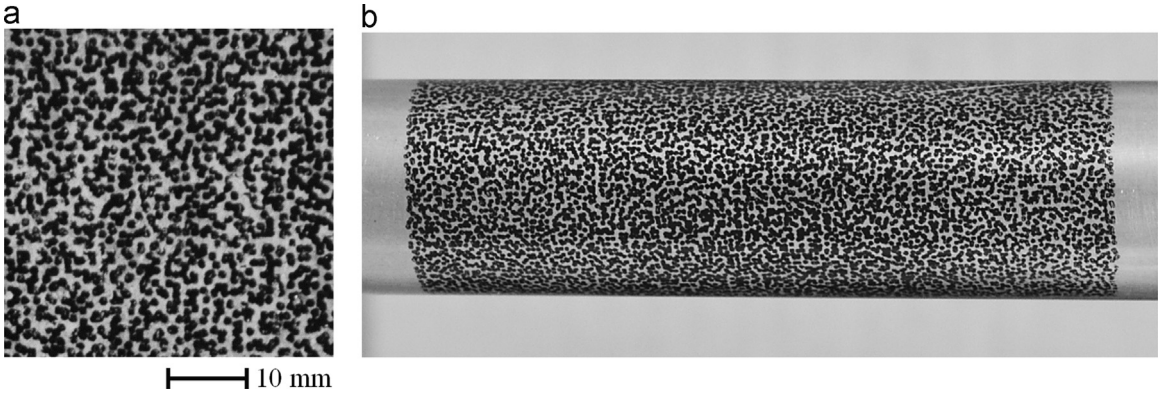

Fig. 5. Speckle pattern produced via toner transfer: (a) on flat concrete surface; and (b) on curved aluminum surface (diameter 16 mm).

on the resulting reference size limits (~10 mm to ~100 mm), it is noted that the proposed toner-transfer technique is applicable to metallic and ceramic specimens typically used in mechanical characterization tests, ranging from tensile coupons (e.g., steel, aluminum, fiber-reinforced cement mortar) to cubes, prisms, beams and cylinders (e.g., cement mortar and concrete).

3.4. Demonstration: mechanical deformations in welded steel plate

The toner-transfer technique is first demonstrated for a quenched and partitioned martensite welded steel plate subjected to uniaxial tensile loading (Fig. 6). The base plate has a rectangular cross section with a width of 9 mm and thickness of 1 mm. The

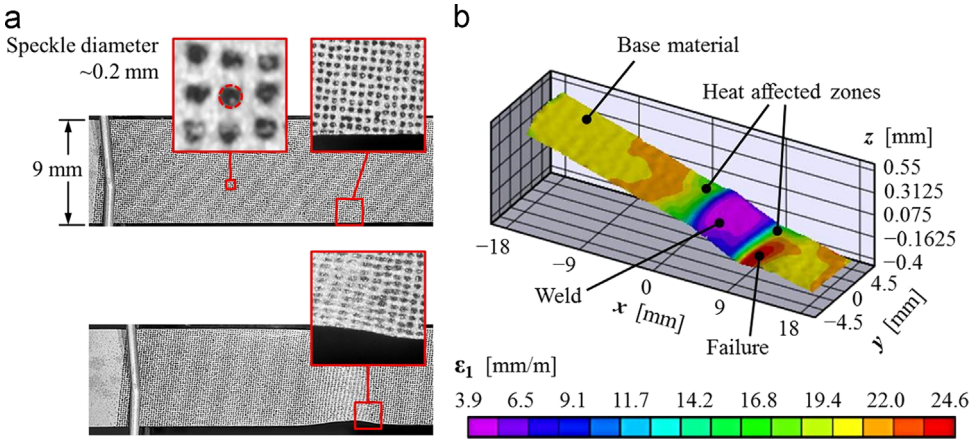

Fig. 6. Tensile testing and DIC analysis of quenched and partitioned steel plate: (a) toner transfer speckle pattern on under elastic (top) and plastic (bottom) deformation; and (b) maximum principal strain map.

measurement area is 9 mm wide and 36 mm long, and includes an approximately 9 mm long weld portion. Images with a resolution of 100 pixel/mm were acquired continuously at a frame rate of 0.5 Hz. Three-dimensional DIC measurement was enlisted to study the influence of the weld on the elasto-plastic response of the plate. The speckle pattern was designed with the minimum speckle diameter of 0.2 mm (i.e., design diameter of 0.05 mm per the tuning plot presented in Fig. 3) to maximize spatial resolution. Prior to impressing the speckle pattern via toner-transfer, the metal surface was sandblasted to obtain a more opaque and light background. The DIC analysis was performed using a subset size of 41×41 pixels and an overlap of 21 pixels.

Fig. 6a shows representative images acquired under elastic and plastic deformation, highlighting the quality of the initial speckle pattern and its ability to deform with negligible degradation (for example because of toner disbond). DIC analysis on the deformed speckle pattern enabled the estimation of the elastic constants of the material in the welded area and the adjacent heat-affected areas, and the elasto-plastic behavior was described by effectively performing DIC measurements until the tensile failure occurred at a load of 9.72 kN. Fig. 6b shows the map of the principal tensile strain, ε_1, on the measurement surface ($-18 \le x \le 18$ mm, $-4.5 \le y \le 4.5$ mm) close to the failure load. The strain contours allow one to clearly recognize the base material, the weld zone ($0 \le x \le 9$ mm), and the crack nucleation region in the heat-affected zone around $x = 9$ mm. In addition, the vertical (z) coordinates in Fig. 6b describe the relatively small out-of-plane deformation of the specimen that developed due to the eccentricity of the tensile force along the weld region.

3.5. Demonstration: thermal deformations in aluminum plate

The effectiveness of the toner-transfer technique is demonstrated for a speckle pattern on a 125×125 mm^2 surface of a 5 mm thick aluminum plate, which was subjected to increasing temperatures between 22 and 451 °C (i.e., 70% of the nominal melting temperature of aluminum). It is noted that the melting temperature of the toner is about 70–90 °C and, since the viscosity is a function of the temperature [25], the toner tends to smudge as the temperature increases, thereby degrading the speckle pattern. Therefore, the experimental demonstration is important also to verify if, and to what extent, toner melting results in a degradation of the toner-transferred speckle pattern. To this end, to simulate a worst-case scenario, the patterned surface was held in a vertical position for the entire duration of the test.

The speckle pattern was designed to obtain 4.5-pixel speckles with a scaling factor of 6.4 pixel/mm. The specimen was placed in a thermally-conductive and transparent glass ceramic container in a laboratory furnace suitable for heat treatments. The furnace temperature was increased in 13 different steps. In each step, the temperature on the measurement surface was measured using a thermocouple. Once stable temperature readings were obtained, the furnace door was opened for a few seconds to facilitate image acquisition and 640 × 480-pixel images were acquired at a frame rate of 200 Hz. It is noted that while the specimen inevitably experienced temperature drops when the oven door was opened, the objective of the experiment was to study pattern degradation as a result of the prolonged exposure to high temperatures in the oven. A blue bandpass (450–490 nm) optical filter was mounted in front of the optics to minimize near-infrared specimen emission effects [29], and the specimen was illuminated with white LED light having an emission spectrum peak lying within the filter bandwidth [30].

To reduce the noise in the reference image [12], 400 frames of the 125×125 mm^2 measurement surface were acquired at the initial temperature of 22 °C, and their average was used as the reference (zero-strain) image. At each temperature step, 400 images were acquired and the resulting DIC strain matrices were averaged element by element to minimize image distortion effects due to the hot air flow [31]. The DIC analysis was performed using a subset size of 21×21 pixels and an overlap of 16 pixels. Fig. 7 shows the resulting average in-plane axial strains, ε_{xx} and ε_{yy}, as a function of the temperature, where the error bars indicate the standard deviation of the average strain matrices. It is noted that the nonlinear trend at temperatures above 250 °C reflects the increase in the linear coefficient of thermal expansion at higher temperatures [32]. It can be seen that the quality and stability of the speckle pattern were allowed to perform the DIC analysis up to the maximum temperature attained, with associated axial strains ε_{xx} and ε_{yy} up to 1.2%, without the need of incremental correlation. Fig. 8 shows two representative images of the speckle pattern, one at a temperature of 22 °C, and one acquired at the end of the three-hour test at a temperature of 451 °C. No visible degradation of the pattern is noted as a result of the exposure to high temperatures. However, a global offset in the image intensity can be seen due to the change of the environmental light after three hours; this is a common problem in DIC measurements and was addressed in the correlation process by implementing a zero-mean normalized cross-correlation [1,2,33].

3.5.1. Quantitative assessment of degradation of speckle pattern

Two parameters were used to quantitatively assess the degradation of the toner-transferred speckle pattern subjected to

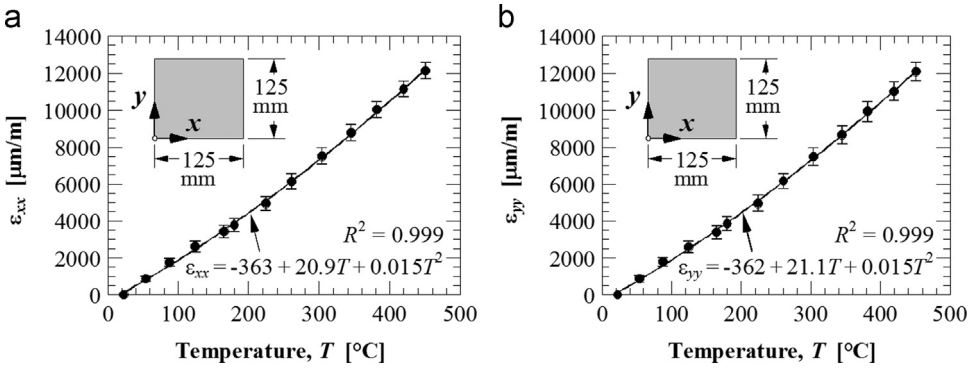

Fig. 7. In-plane thermal deformation of aluminum plate from DIC analysis using toner transfer speckle pattern: (a) axial strain in x-direction, ε_{xx}; and (b) axial strain in y-direction, ε_{yy}.

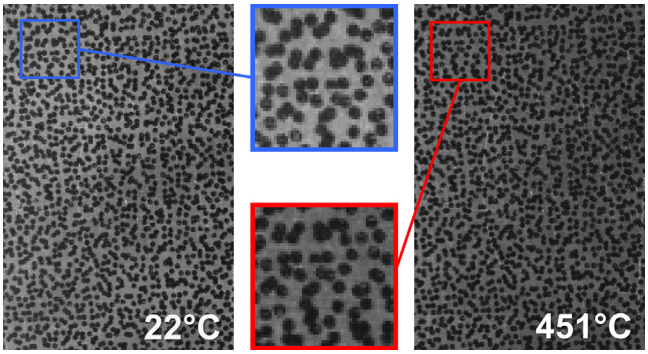

Fig. 8. Toner-transfer speckle pattern on aluminum surface exposed to temperature of 22 and 451 °EC (300 × 200 pixel samples and 50 × 50 pixel close-ups).

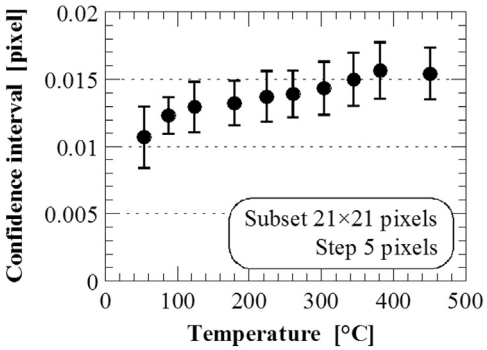

Fig. 9. Confidence interval as function of exposure temperature.

increasing temperatures. The first parameter is the confidence interval [34], which is a measure of the uncertainty in the correlation and was computed using the DIC analysis software Vic-2D 2009 (Correlated Solutions, Inc., Columbia, SC). Since a degrading speckle pattern would yield increasing confidence intervals, the stability of or a marginal increase in the confidence interval can be used as a criterion to monitor degradation as a result of exposure to high temperatures. The second parameter is the previously introduced MIG coefficient [3], which can serve as a complementary parameter to assess the quality of the speckle pattern. In fact, a decrease in MIG coefficient would indicate that the pattern is becoming less effective for DIC analysis. It is noted that, by itself, the stability of or a marginal decrease in the MIG coefficient indicates that the speckle pattern remains effective for DIC analysis, even when it may be deteriorating somewhat.

In Fig. 9, the mean confidence interval and the associated standard deviation are plotted as a function of the exposure temperature (up to 451 °C). For each temperature step, one image is considered and the confidence interval is computed for each 21 × 21 pixel subset, using the image acquired at ambient tem-perature (22 °C) as the reference one (i.e., with a confidence interval equal to zero). The resulting mean confidence interval ranges between 0.0106 pixels at 54 °C and 0.0154 pixels at 451 °C, with no clear increase in standard deviation. Therefore, the uncertainty in displacement measurement increases but remains of the order of 0.015 pixels, thus indicating a negligible degrada-tion of the speckle pattern at exposure temperatures up to 451 °C.

The MIG coefficient [3] is sensitive to changes in the lighting conditions. Therefore, a zero-normalization of the pixel brightness was performed prior to computing the MIG coefficient. For a given acquired image, each 21 × 21 pixel subset was extracted and zero-normalized by subtracting the average intensity value, and dividing the result by the intensity standard deviation as per Eq. (3):

$$S_N(i,j) = \frac{S(i,j) - \overline{S}}{\sigma_S} \tag{3}$$

where $S_N(i,j)$ and $S(i,j)$ are the zero-normalized and the original intensity value of a pixel of a $(2M+1) \times (2M+1)$ squared subset, respectively; σ_S is the intensity standard deviation; and the associated average subset intensity $\overline{S}$ is given as

$$\overline{S} = \frac{1}{(2M+1)^2} \sum_{i=-M}^{M} \sum_{j=-M}^{M} S(i,j) \tag{4}$$

$$\sigma_S = \sqrt{\frac{1}{(2M+1)^2 - 1} \sum_{i=-M}^{M} \sum_{j=-M}^{M} \left[S(i,j) - \overline{S}\right]^2} \tag{5}$$

Then, the MIG coefficient was computed for each zero-normalized subset. Through this approach, the average MIG value of the about 5000 normalized subsets and the associated variability range are computed, thereby enabling the quantitative assessment of the quality of the speckle pattern under varying lighting conditions. The average MIG value of the zero-normalized subsets and the associated standard deviation are plotted as a function of the exposure temperature in Fig. 10. As a result of the zero-normalization process, the average MIG values have a different order of magnitude compared with those obtained without the need of zero-normalization, such as in the case illustrated in Fig. 4. By comparing the average MIG values between 22 and 451 °C, it is evident that the differences between the average values at different temperatures are negligible compared with the MIG variability at a given temperature.

The evidence obtained through the analysis of the confidence interval and MIG coefficient highlights the potential of the proposed technique for a broad range of metallic specimens and

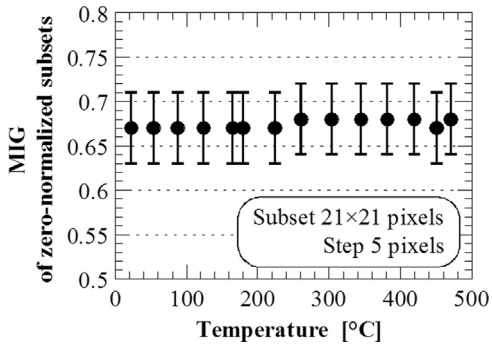

Fig. 10. MIG of zero-normalized subsets as function of exposure temperature.

elevated temperature tests. However, since printer toners typically melt at about 70–90 °C and their viscosity is strongly dependent on the temperature [25], the suitability of a given measurement surface, toner and speckle pattern should be verified on a case-by-case basis.

4. Conclusions

This paper introduces a novel thermo-mechanical toner-transfer technique to impress speckle patterns of higher quality and repeatability compared with those obtained through spray painting using airbrushes. First, the desired speckle pattern is numerically designed and tuned with respect to speckle size and spacing. Then, the pattern is printed on suitable paper and transferred onto the measurement surface by simultaneously applying heat and pressure, for example using a flatiron.

A tuning procedure to compensate for the difference in size between nominal (design) and impressed (toner-transferred) speckle pattern has been demonstrated. Based on the mean intensity gradient coefficient computed from the resulting speckle pattern impressed on aluminum surfaces in four different scales, it has been shown that an improved quality can be consistently attained compared with spray-painted patterns.

The technique is suitable only for surface materials that can be heated to about 100 °C for a few minutes, such as metallic alloys and cement composites. Examples of applications on flat concrete and curved aluminum surfaces have been presented. Based on the allowable dimensions of the framed area, the toner-transfer technique lends itself to applications on numerous standard metallic and ceramic specimens used for the characterization of mechanical and thermal properties.

Proof of concept has been demonstrated for the case of a quenched and partitioned welded steel plate subjected to tensile loads up to failure, and for an aluminum plate exposed to temperatures up to 70% of the melting point. The speckle patterns obtained via toner transfer have been shown to negligibly degrade under large deformations as well as temperatures that are far in excess of those associated with melting of the toner, allowing to perform accurate DIC measurements irrespective of the mechanical and thermal load imparted.

Acknowledgments

The collaborative research presented herein was made possible through the support of the Politecnico di Milano (Milan, Italy) and the College of Engineering and Computing at the University of South Carolina (Columbia, SC).

References

[1] Sutton MA, Orteu J-J, Schreier HW. Image correlation for shape, motion and deformation measurements. New York, NY: Springer; 2009.
[2] Pan B, Qian K, Xie H, Asundi A. Two-dimensional digital image correlation for in-plane displacement and strain measurement: a review. Meas Sci Technol 2009;20:062001.
[3] Pan B, Lu Z, Xie H. Mean intensity gradient: an effective global parameter for quality assessment of the speckle patterns used in digital image correlation. Opt Laser Eng 2010;48:469–77.
[4] Lecompte D, Smits A, Bossuyt S, Sol H, Vantomme J, Van Hemelrijck D, Habraken AM. Quality assessment of speckle patterns for digital image correlation. Opt Laser Eng 2006;44:1132–45.
[5] Zhou P, Goodson KE. Subpixel displacement and deformation gradient measurement using digital image/speckle correlation (DISC). Opt Eng 2001;40:1613–20.
[6] Lecompte D, Sol H, Vantomme J, Habraken A. Analysis of speckle patterns for deformation measurements by digital image correlation. Proc. SPIE 2006;6341:63410E.
[7] Pan B, Qian K, Xie H, Asundi A. On errors of digital image correlation due to speckle patterns. Proc. SPIE 2009;7375:73754Z.
[8] Bornert M, Brémand F, Doumalin P, Dupré J-C, Fazzini M, Grédiac M, Hild F, Mistou S, Molimard J, Orteu J-J, Robert L, Surrel Y, Vacher P, Wattrisse B. Assessment of digital image correlation measurement errors: methodology and results. Exp Mech 2009;49:353–70.
[9] Mazzoleni P, Matta F, Zappa E, Sutton MA, Cigada A. Gaussian pre-filtering for uncertainty minimization in digital image correlation using numerically-designed speckle patterns. Opt Laser Eng 2014;66:19–33.
[10] Yaofeng S, Pang JHL. Study of optimal subset size in digital image correlation of speckle pattern images. Opt Laser Eng 2007;45:967–74.
[11] Pan B, Xie H, Wang Z, Qian K, Wang Z. Study on subset size selection in digital image correlation for speckle patterns. Opt Express 2008;16:7037–48. Wang
[12] YQ, Sutton MA, Bruck HA, Schreier HW. Quantitative error assessment in pattern matching: effects of intensity pattern noise, interpolation, strain and image contrast on motion measurements. Strain 2009;45:160–78.
[13] Rivolta B, Silvestri A, Zappa E, Garghentini A. 5083 aluminum alloy welded joints: measurements of mechanical properties by DIC. J ASTM Int 2012;9 JAI104307, http:/dx.doi.org/10.1520/JAI104307.
[14] Bolzon G, Buljak V, Zappa E. Characterization of fracture properties of thin aluminum inclusions embedded in anisotropic laminate composites. Fract Struct Integr 2012;19:20–8.
[15] Ghorbani R, Matta F, Sutton MA. Full-field deformation measurement and crack mapping on confined masonry walls using digital image correlation. Exp Mech 2015;55(1):227–43.
[16] Matta F, Mazzoleni P, Zappa E, Sutton MA, ElBatanouny MK, Larosche AK, Ziehl P. Shear strength of FRP reinforced concrete beams without stirrups: verification of fracture mechanics formulation. In: Lopez M, Carloni C, editors. ACI special publication 286 – a fracture approach for FRP – concrete structures. Farmington Hills, MI: American Concrete Institute; 2012. p. 13 CD-ROM #SP-286–6.
[17] Gencturk B, Hossain K, Kapadia A, Labib E, Mo Y-L. Use of digital image correlation technique in full-scale testing of prestressed concrete structures. Measurement 2014;47:505–15.
[18] Helm JD. Digital image correlation for specimens with multiple growing cracks. Exp Mech 2008;48:753–62.
[19] El-Hajjar RF, Petersen DR. Adhesive polyvinyl chloride coatings for quantitative strain measurement in composite materials. Compos B–Eng 2011;42:1929–36.
[20] Collette SA, Sutton MA, Miney P, Reynolds AP, Li X, Colavita PE, Scrivens WA, Luo Y, Sudarshan T, Muzykov P, Myrick ML. Development of patterns for nanoscale strain measurements: I. Fabrication of imprinted Au webs for polymeric materials. Nanotechnology 2004;15:1812–7.
[21] Scrivens WA, Luo Y, Sutton MA, Collette SA, Myrick ML, Miney P, Colavita PE, Reynolds AP, Li X. Development of patterns for digital image correlation measurements at reduced length scales. Exp Mech 2007;47:63–77.
[22] Li J, Xie H, Luo Q, Gu C, Hu Z, Chen P, Zhang Q. Fabrication technique of micro/nano-scale speckle patterns with focused ion beam. Sci China – Phys Mech Astron 2012;55(6):1037–44.
[23] Liu ZW, Xie HM, Fang DN, Dai FL, Wang WN, Fang Y. Artificial submicron or nanometer speckle fabricating technique and electron microscope speckle photography. Rev Sci Instrum 2007;78:033101.
[24] Yang XB, Liu ZW, Xie HM. A real time deformation evaluation method for surface and interface of thermal barrier coatings during 1100 °C thermal shock. Meas Sci Technol 2012;23(10):105604.
[25] Hartus T. Adhesion of electrophotographic toner on paper. Graph Arts Finl 2001;30(3):14–9.
[26] Gonzalez RC, Woods RE. Digital image processing. 3rd ed.. Upper Saddle River, NJ: Prentice-Hall; 2007.
[27] American Society for Testing and Materials. Standard test method for compressive strength of cylindrical concrete specimens – ASTM C39/C39M-14a. West Conshohocken, PA: ASTM International; 2014.
[28] American Society for Testing and Materials. Standard test method for static modulus of elasticity and Poisson's ratio of concrete in compression – ASTM C469/C469M-14. West Conshohocken, PA: ASTM International; 2014.

[29] Pan B, Wu D, Xia Y. An active imaging digital image correlation method for deformation measurement insensitive to ambient light. Opt Laser Technol 2012;44:204–9.
[30] Narukawa Y. White-light LEDs. Opt Photonics News 2004;15:24–9.
[31] Lyons JS, Liu J, Sutton MA. High-temperature deformation measurements using digital-image correlation. Exp Mech 1996;36:64–70.
[32] Spittel M, Spittel T. Mechanical properties of light metal alloys. In: Warlimont H, editor. Landolt-Börnstein – Group VIII advanced materials and technologies, volume 2: materials, subvolume C: metal forming data, Part 2: non-ferrous alloys – light metals. Heidelberg, Germany: Springer; 2011. p. 74–6.
[33] Tong W. An evaluation of digital image correlation criteria for strain mapping applications. Strain 2005;41:167–75.
[34] Correlated Solutions, Inc. Vic-2D reference manual. Columbia, SC: Correlated Solutions, Inc. ⟨http://www.correlatedsolutions.com/installs/Vic-2D-2009-Manual.pdf⟩; 2009 [accessed 08.05.15].